3º Seminário Internacional Torres Vedras (Portugal) April 29-30, 2010
Hydrogen Energy and Sustainability- Advances in Fuel Cells and Hydrogen Workshop

Degradation of Lithium Iron Phosphate-based Cathode in Lithium-ion Batteries: A *Post-mortem* Analysis

M.J. Plancha[1], C.M. Rangel[1]
B. Rodrigues[2], F. Azevedo[2]

[1]Laboratório Nacional de Energia e Geologia, Unidade de Pilhas de Combustível e Hidrogénio,
Estrada do Paço do Lumiar 22, 1649-038 Lisboa, Portugal
mjoao.plancha@ineti.pt carmen.rangel@ineti.pt

[2]A.A. Silva, S.A.-Autosil, Edif. Komax, Estrada Nacional 249-4, Trajouce
2785-034 S. Domingos de Rana, Portugal
www.autosil.pt

Abstract

Commercial Li-ion batteries were studied in view to investigate the degradation of the positive electrode in an end-of-life battery condition. *Post-mortem* analyses were performed by using SEM and DRX techniques; structural and morphological changes after prolonged cycling were evaluated comparatively to a fresh cathode sample. The cycling procedure based on a constant current (CC)/constant voltage (CV) charge and CC discharge was executed, being the condition of end-of-life battery achieved after submitting the Li-ion battery to nearly 2000 charge/discharge cycles. EDS analysis revealed zirconium element as the dopant of a $LiFePO_4$-based cathode of the battery under study. According to X-ray diffraction results for the fresh (charged condition) cathode, the positive electrode includes in its constitution a mixture of crystalline compounds, $LiFePO_4$ and $FePO_4$. SEM images displayed and DRX patterns obtained for the cycled cathode showed modifications compared to the fresh cathode results, evidencing the degradation of the battery at the end-of-life: decrease in the density of microparticles associated to areas where the insertion/de-insertion occurs; decrease of the $LiFePO_4/FePO_4$ ratio; both results pointed out to the occurrence of battery loss capacity with the imposed charge/discharge cycles.

Keywords: *Cathode degradation, Lithium-ion batteries, Lithium iron phosphate, Charge/discharge cycles*

1 Introduction

Lithium-ion batteries, first introduced by Sony in 1991 [1], have come to invade the market to replace Ni-Cd and Ni-MH batteries, particularly in applications such as portable telephones, computers and other devices, which usually utilize rechargeable batteries. World production of Li batteries came to 500 million units in 2000, and is bound to reach 4.6 billion in 2010 [2].

Besides consumer electronics, the use of lithium ion-batteries is rapidly increasing in the automotive, aerospace and defense sectors due to its energy density. Next generation cars are likely to be powered by a combination of batteries, fuel cells and capacitors in hybrid system configurations that allow battery charging. No energy storage device by itself actually satisfies the demands of automotive applications [3].

Apart from the high energy density achieved, other major advantages of using Li-ion batteries are the low rate of self-discharge and excellent charge/discharge life cycles. In addition, these batteries are environmentally acceptable. Whatever the technology used in its manufacture, the performance characteristics are related to the intrinsic properties of the electrode's materials.

The useful life cycles of charge/discharge and the total lifetime of the batteries (mentioned cycles and in rest period), are dependent on the nature of the interfaces between the electrodes and electrolyte, while safety is a function of stability of materials electrode and interfaces. The optimal combination of the group electrode-electrolyte-electrode can only be

achieved through selective use of existing and new materials for the positive and negative electrodes, and the proper combination with the electrolyte, so as to minimize adverse reactions related to the interface electrode-electrolyte (critical phase of any electrochemical system).

In lithium-ion batteries, since the anode material is carbon, not containing lithium, the positive electrode (cathode) must act as a source of ions of this metal, thus requiring intercalation compounds based on lithium, stable in air, in order to facilitate the cell assembly. The most common cathode materials are lithium cobalt oxides ($LiCoO_2$), lithium nickel oxides ($LiNiO_2$), lithium manganese oxides such as $LiMnO_2$ and $LiMn_2O_4$, etc. In Table 1 some characteristics of cathode materials for lithium-ion batteries are depicted.

Table 1. Characteristics of cathode materials in lithium-ion batteries.

Electrode material	Nominal voltage (V)	Life cycles number	Specific charge* (Ah/Kg)
$LiCoO_2$	3.7	400	137
$LiMn_2O_4$	3.7	800	148
$LiFePO_4$	3.2	2000	170

* Theoretical

Initially, it was considered the use of the compound with a layered structure, the $LiNiO_2$, as it displayed a higher specific capacity (192 $AhKg^{-1}$) compared to $LiCoO_2$ [4, 5]. Afterwards, the substitution of the Ni ions for the Co ion was adopted in order to provide a solution to safety problems (reaction with the electrolyte). $LiCoO_2$ widely used in commercial Li-ion batteries is however an expensive material and requires an electronic circuit to prevent, in the charging process, overcharging where the battery is inserted [6]. This risk also limits the size of the batteries.

In 1997, a research group at the University of Texas proposed a cathode material never used before, $LiFePO_4$, cheaper and safer than lithium cobalt oxide, the most common cathode material in the market. Lithium iron phosphate with an ordered olivine-type structure, belongs to a general class of "polyanion" compounds containing compact tetrahedral "anion" structural units $(XO_4)^{n-}$ (X = P, S, As, Mo or W) with strong covalent bonding in the lattice, to produce higher coordination sites such as oxygen octahedra that are occupied by other metal ions. Other phosphates of lithium and transition metal such as Mn, Ni or Co have also been the subject of studies due to their high theoretical specific capacity ($170mAhg^{-1}$) [7]. However, $LiFePO_4$ is the most attractive due to its high stability, low cost and high compatibility with the environment (low toxicity). This compound has also a high lithium intercalation voltage (~ 3.5V vs. Li) and is easily synthesised [8]. Despite all these advantages, the full capacity of $LiFePO_4$ is difficult to be achieved, since its electronic conductivity is very low [9], which leads to initial capacity loss and to slow diffusion of Li^+ ion in the olivine structure [10]. At a lattice scale, mixed electronic and ionic conductivity is required to preserve the neutrality of the total charge during the lithium-ion transport, being the chemical diffusion coefficient rate-limited by the slowest species. One of the ways used for improving the electronic conductivity of these materials is the selective doping of $LiFePO_4$ by multivalent cations such as Al^{3+}, Nb^{5+} and Zr^{4+}. This process was first made at the Massachusetts Institute of Technology, by Chiang and colleagues, which showed that the electronic conductivity of lithium iron phosphate has increased 10 million times in relation to the conductivity of the undoped material, reaching up to 10^{-2} Scm^{-1} at room temperature [11]. The electronic conductivities obtained are far superior to other commonly used cathodes such as $LiCoO_2$ (~ 10^{-3} Scm^{-1}) and $LiMn_2O_4$ ($2x10^{-5}$ to $5x10^{-5}$ Scm^{-1}). The resulting doped $LiFePO_4$ materials have storage capabilities that are close to the theoretical limit of 170 $mAhg^{-1}$ at low charge/discharge rates.

In this paper, the degradation of Li-ion battery cathodes based on $LiFePO_4$ was evaluated by means of a *post-mortem* analysis done to a battery sample in the end of life and comparing it with the results obtained in a fresh cathode sample in the charged condition (without any charge/discharge cycle). The failure analysis was conducted by using SEM (Scanning Electron Microscopy) coupled with EDS (Energy Dispersion Spectroscopy) and X-ray diffraction on samples selected from the cathodes of batteries before and after charge/discharge cycles.

2 Experimental

Commercial Li-ion batteries with nominal voltage of 3.2V and having a graphite type negative electrode and a cathode based in lithium iron phosphate were subjected to ~2000 charge/discharge cycles in order to obtain an end-of-life condition. A series of four batteries were first discharged at 20A during 1 hour (constant current protocol). Afterwards, continuous cycles of charge/discharge were performed with a time interval of 5 minutes between each charge and discharge step. The charges were done at a current density of 10A and a maximum voltage of 14.5V for 3 hours under constant current-constant voltage (CC-CV) condition. The part of the cycle corresponding to

the discharge of the batteries was carried out at the same conditions of the first one.

Cycled and fresh (in charged state) cylindrical Li-ion batteries (schematically illustrated in figure 1) were manually dismantled in a fume-hood. After removal of the steel case at atmospheric pressure, the batteries were left to stand for 1 h in a vacuum system. The samples were then manually fully disassembled (unrolled) in an Ar filled gloves box, allowing recognition and separation of the components (cathodes, anodes, plastic cases, steel cases, copper foils, polymer foils and electrical contacts).

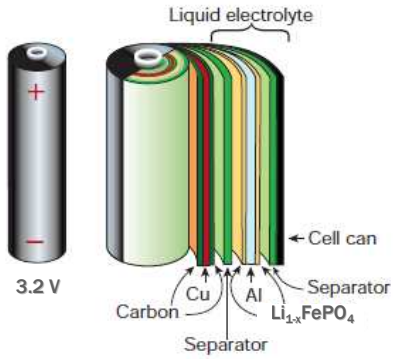

Fig. 1. Schematic drawing of the Li-ion batteries under study, showing the structure, components and shape. Adapted from ref. 5.

The analyses of cathode samples before and after charge/discharge cycles were done by using Scanning Electron Microscopy (SEM), coupled with Energy Dispersion Spectroscopy (EDS) using a Phillips XL 30 Model FEG scanning electron microscope at 2kV (to minimize charging of the uncoated samples), equipped with an energy dispersive X-ray detector.

X-Ray Diffraction (DRX) measurements were also carried out, using a Rigaku model D/Max III C automated diffractometer with graphite monochromated Cu radiation. Data were collected in the 2θ range from 5 to 105º at a scan rate of $1.2^{o}min^{-1}$.

3 Results

3.1 Battery cycling

Charge/discharge cycles were performed for a series of four batteries. Typical results for one complete cycle after the discharge of the batteries is shown in Figure 2.

The voltage variation profiles obtained by constant current discharge and charge steps are shown, together with the current profile during the potentiostatic charge (constant voltage polarisation).

As expected, the voltage value of the battery system decreases during the discharge (till about 10.5V in the first and second discharges observed in the figure) and increases during the galvanostatic charge. In this step, when voltage value reaches 14.5V, the switch to constant voltage charge (at 14.5V) is done.

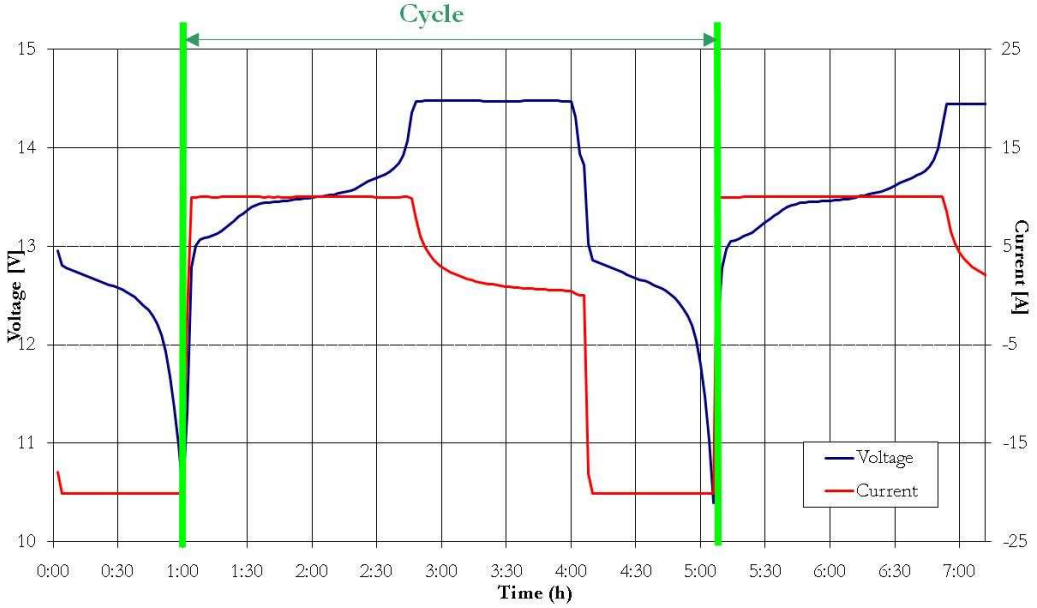

Fig. 2. Voltage and current variations with time in the charge/discharge cycling of the Li-ion based batteries used in this work. The graph shows data for four batteries connected in series.

3.2 SEM and EDS analyses

In order to observe morphological changes associated to the positive electrode and also to detect any eventual elemental composition change, SEM/EDS analyses were carried out on samples taken from a fresh and a cycled battery cathode.

SEM micrographs of the samples obtained at a magnification of 5000 X are shown in Figures 3 and 4 respectively. It can be seen the presence of crystal aggregates together with the presence of some binder. The aggregates are formed by microparticles with irregular shape and various sizes (typically 0.5 to 1µm and some with ~2µm), which assure a high specific area, and micropores, which allow the diffusion of the electrolyte to inner regions of the electrode. The battery cycled sample (figure 4) shows some changes in morphology.

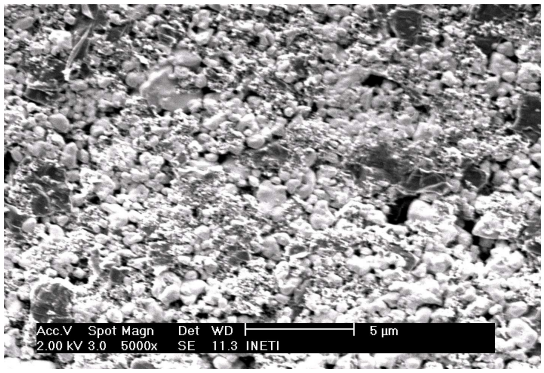

Fig. 3. SEM micrograph of the fresh cathode sample (in charged condition).

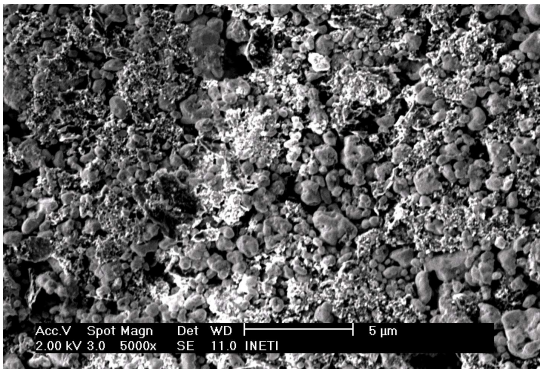

Fig. 4. SEM micrograph of the cathode sample of a cycled battery.

After the cycles, the amount of micropores seems to increase and to enlarge; simultaneously, the quantity of microparticles decreases. This may be indicative of an area decrease of the regions where the insertion/de-insertion takes place, bringing as a consequence a decrease of the battery capacity.

The results of EDS analyses made to the cathode's samples (figure 5) are consistent with the fact that the cathode of the Li-ion battery is based on a lithium iron phosphate, with zirconium metal ions as dopant, making it a compound of general formula $LiFe_xZr_{1-x}P_yO_z$.

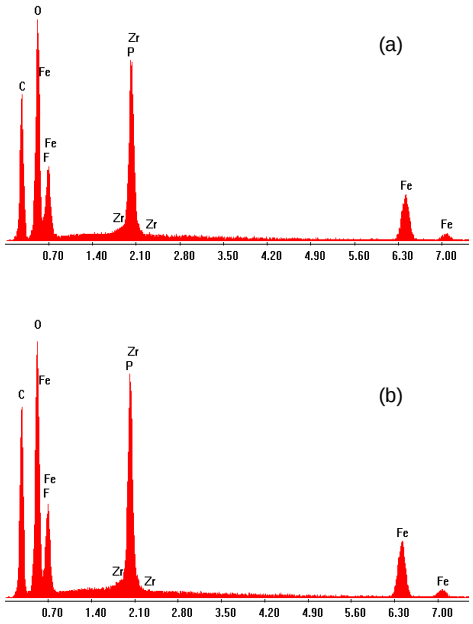

Fig. 5. EDS spectra correspondent to area analyses of sample cathodes shown in Fig. 3 and 4: fresh (a) and cycled (b).

3.3 XRD analyses

X-ray diffraction analysis was employed to evaluate the crystal structure of the cathodes and identify any structural or crystalline composition changes with the cycling.

Figure 6 shows the X-ray diffraction pattern for the sample of the fresh cathode. The overall pattern (with the presence of various sharp peaks) indicates a relatively high degree of crystallinity. Diffraction peaks were identified as belonging to two crystalline compounds: iron phosphate, $FePO_4$ [12] and lithium iron phosphate, $LiFePO_4$ - "triphylite" [13]. The diffraction peak marked "C" in the figure, refers to graphite, which is part of the Li-ion battery composite cathode. In Figure 7 is presented the XRD pattern for the sample corresponding to the cycled cathode battery.

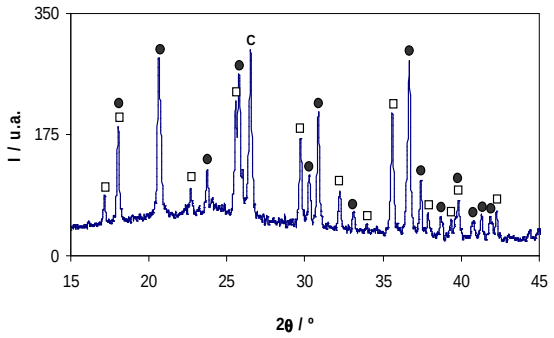

Fig. 6. X-ray diffraction pattern for the fresh cathode sample of the Li-ion battery under study. Compounds identified are: $FePO_4$ (●) and $LiFePO_4$ (□).

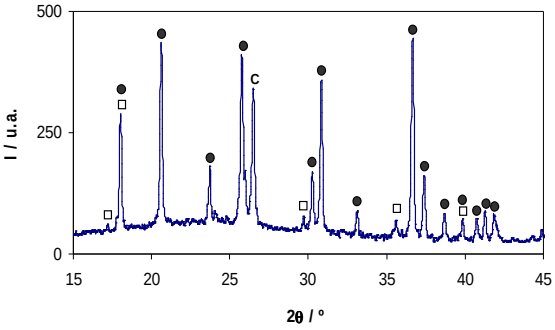

Fig 7. X-ray diffraction pattern for the cycled cathode sample of the Li-ion battery under study. Compounds identified are: $FePO_4$ (●) and $LiFePO_4$ (□).

Similarly, the cathode battery after charge/discharge cycles presents a high crystallinity degree. It appears that no distinct structural modification exists as no change in peak position is observed when comparing with the fresh sample. It is noted, however, an increase in the proportion between the intensity values of the iron phosphate characteristic peaks and those of the $LiFePO_4$ peaks for the cycled cathode, comparatively to the same diffraction peaks proportion of the fresh cathode. This might be indicative that the amount of lithium iron phosphate has decreased. Also, in the cycle discharge steps the intercalation of lithium turns sluggish with time and the conversion of $FePO_4$ for the lithiated form is only partially accomplished affecting the capacity of the battery.

4 Conclusions

- Cathode EDS analysis is consistent with a cathode composition based on lithium iron phosphate.
- The cathode is doped, for higher conductivity, with zirconium metal ions, making the battery's positive electrode mainly consisting in a compound of general formula $LiFe_xZr_{1-x}P_yO_z$.
- The cathode is shown to have been modified with the imposed charge/discharge cycles. Changes were observed either in the morphology, either in the proportion of the existing crystalline compounds, the iron phosphate and the lithium iron phosphate.
- The cathode microparticles regions decreased with the battery cycling indicating degradation of the electrochemical active area of the cathode.
- Battery capacity also decreases as the conversion of $FePO_4$ to the lithiated form is only partially achieved in the discharge cycle step.

References

[1] M.B.J.G. Freitas and E.M. Garcia, *J. Power Sources* 171 (2007) 953.

[2] UMICORE, Materials Technology Group, http://www.umicore.com.

[3] Garry Golden, "Hydrogen storage could support lithium ion batteries in electric vehicles", 2008, http://www.theenergyroadmap.com.

[4] A. Patil, V. Patil, D.W. Shin, J.-W. Choi, D.-S. Paik and S.-J. Yoon, *Mater. Res. Bull.* 43 (2008) 1913.

[5] J.-M. Tarascon and M. Armand, *Nature* 414 (2001) 359.

[6] *Science News* 158 (2000) 399.

[7] A.K. Padhi, K.S. Nanjundaswamy and J.B. Goodnough, *J. Electrochem. Soc.* 144 (1997) 1188.

[8] J. Chen, M.J. Vacchio, S. Wang, N. Chernova, P.Y. Zavalij and M.S. Whittingham, *Solid State Ionics* 178 (2008) 1676.

[9] A.S. Andersson, B. Kalska, L. Häggström and J.O. Thomas, *Solid State Ionics* 130 (2000) 41.

[10] B. Jin and H.-B. Gu, *Solid State Ionics* 178 (2008) 107.

[11] S.-Y. Chung, J.T. Bloking and Y.-M. Chiang, *Nature Materials* 1 (2002) 123.

[12] JCPDS Card nº 70-6685 (Powder Diffraction File, International Center for Diffraction Data, Swarthmore, PA).

[13] JCPDS Card nº 81-1173 (Powder Diffraction File, International Center for Diffraction Data, Swarthmore, PA).